Evaluation of polarisation angle diversity technique for reliable wireless communication in highly electromagnetic scattered environment

A Project Report

submitted by

VALLURI SAIKIRAN

in partial fulfilment of the requirements
for the award of the degree of

MASTER OF TECHNOLOGY

DEPARTMENT OF ELECTRICAL ENGINEERING
INDIAN INSTITUTE OF TECHNOLOGY MADRAS.

MAY 2014

THESIS CERTIFICATE

This is to certify that the thesis titled **Evaluation of polarisation angle diversity technique for reliable wireless communication in highly electromagnetic scattered environment**, submitted by **Valluri Saikiran**, to the Indian Institute of Technology, Madras, for the award of the degree of **MASTER OF TECHNOLOGY**, is a bona fide record of the research work done by him under our supervision. The contents of this thesis, in full or in parts, have not been submitted to any other Institute or University for the award of any degree or diploma.

Dr. David Koilpillai
Research Guide
Professor
Dept. of Electrical Engineering
IIT-Madras, 600 036

Dr. Devendra Jalihal
Research Guide
Professor
Dept. of Electrical Engineering
IIT-Madras, 600 036

Dr. Radha Krishna Ganti
Research Guide
Assistant Professor
Dept. of Electrical Engineering
IIT-Madras, 600 036

Place: Chennai

Date: 4th May 2014

ACKNOWLEDGEMENTS

I would like to express my greatest gratitude for the people who have helped and supported me throughout my project. I am grateful to my guides, Dr. David Koilpillai and Dr. Devendra Jalihal, for their continuous support. This project would not have been a success without their valuable suggestions and insights. Despite their busy schedule they always managed time to discuss the issues and guide the project in a proper course.

I would like to thank Dr.Radhakrishna Ganti,professor involved in the project, for his time and again feedback and immense help in our work.

I would also like to thank Dr.Ken Takei, senior engineer in Hitachi Research and Development labs, Japan, on whose innovative idea the project is based upon, for his regular supervision and immense support in the project.I would also like to thank my project partner, Konduri Sriram for his friendly support.

Last but not the least, I express my sincere thanks to all the staff members of different labs who have been more than helpful in performing experiments.They were always ready to supply additional equipment required for performing experiments efficiently for collecting measurements.

ABSTRACT

A radio architecture was proposed by the Hitachi laboratories, Japan, for reliable wireless communication in highly electromagnetic scattered environment.This thesis describes the various experiments carried out and measurements obtained.The preliminary experimental setup was implemented using two Universal Software Radio Peripherals(USRPs) and a MIMO expansion cable for synchronising them at transmitter and a USRP at receiver.400 MHz custom antennas were used at transmitter and receiver.

This thesis describes the signal processing view of the proposed technique.The detailed explanation for the proposed transceiver architecture,the transmitted and received signal projections and the technical specifications of the implementation are given.It also describes the preliminary experimental setup and the technical challenges involved in performing the experiments and the steps taken to mitigate them.

The transmitter and receiver algorithms used are explained step to step.The analysis results of the collected data are explained clearly and are compared with the single antenna transceiver results,thus, bringing out the flavour of the advantage of the proposed technique over the traditional wireless communication methods.Performance evaluation of the receiver algorithm and the chip error probability curve are also mentioned.

The Project Team

The Hitachi team that took part in the experiment had the following members:

1. Dr. Ken Takei, chief designer and overall incharge

2. Mr. Aono, Engineer

3. Mr. Kawakami, Engineer

The IITM team consisted of the following:

1. Prof. Radhakrishna Ganti

2. Prof. David Koilpillai

3. Prof. Devendra Jalihal

4. Mr. Saikiran Valluri, Student

5. Mr. Sriram Konduri, Student

TABLE OF CONTENTS

LIST OF FIGURES

CHAPTER 1

INTRODUCTION

1.1 Project background

Even to this day, reliable machine to machine(M2M) communication in industries with large electromagnetic scatterers is established using wired communication. Wireless communication cannot be relied upon due to the highly non-line-of-sight multipath propagation channel in industries. Also the environment in industries is static and is of extremely slow fading type. If the signal is in deep fade it continues to be in deep fade for a very long time. But wired communication has certain disadvantages regarding security of the equipment as the wiring used can be intentionally or unintentionally damaged.

A radio architecture [1] was proposed by the Hitachi laboratories, Japan, for wireless monitoring and control of infrastructure equipment in industries.The proposed architecture is useful for reliable machine-to-machine(M2M) communication using non-line-of-sight waves which are reflected by electromagnetic scatterers.The proposed radio transmits the signal, which is expanded by orthogonal codes, on different wireless paths using different polarisation directions at different times.

This approach results in good resistance against outer interferences and unexpected interruption in highly electromagnetic scattered environment, which enables it to achieve highly-reliable wireless communication,which is inevitable in industries. Also this approach converts the very slow fading channel to fast fading channel so that the signal is relatively not in deep fades, thus resulting in low BERs.

This technique of polarisation angle diversity, proposed by the Hitachi for reliable M2M communications was studied theoretically.Various transmitter diversity schemes, [2] and [3] were studied.These schemes were compared with the proposed technique on

the grounds of inducing fast fading by polarisation angle diversity and Doppler fading. Then a contract was established between the Hitachi and Indian Institute of Technology, Madras team for the evaluation of reliability and feasibility of the technique in wireless M2M communication.

Initially the following method for attaining polarisation angle diversity was proposed by the Hitachi.Let us suppose $a(t)$ is the signal to be transmitted.$a(t)$ is digitally up-converted to 435 and 435.1 MHz in order to generate $A(t)$ and $B(t)$ respectively.These resultant signals are manipulated and sent to the transmitter antennas as illustrated. Here, $\omega_1 = 435MHz$ and $\omega_2 = 435.1MHz$. The transmitted signal through vertical

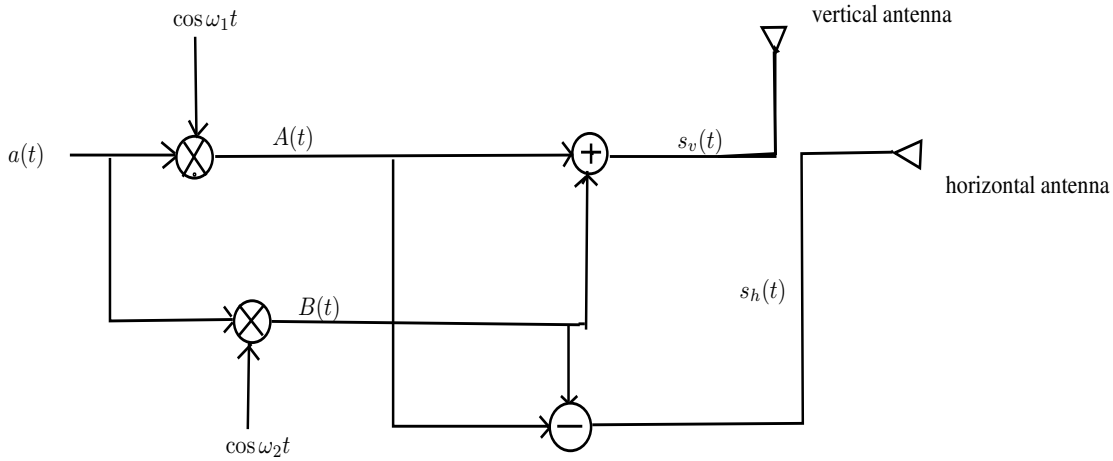

Figure 1.1: Schematic of the proposed transmitter

antenna,

$$s_v(t) = a(t)(\cos\omega_1 t + \cos\omega_2 t) = 2a(t)\cos(\frac{\omega_1-\omega_2}{2})t\cos(\frac{\omega_1+\omega_2}{2})t,$$

and the signal through horizontal antenna,

$$s_v(t) = a(t)(\cos\omega_1 t - \cos\omega_2 t) = 2a(t)\sin(\frac{\omega_2-\omega_1}{2})t\sin(\frac{\omega_1+\omega_2}{2})t.$$

This technique results in the formation of spacial beats of electromagnetic waves of frequency, $\frac{\omega_2-\omega_1}{2} = 50KHz$.The transmitted electromagnetic vector rotates through 360 degrees with a frequency of 50 KHz. The receiver schematic is shown in fig.1.2.At the receiver, the received vertical and horizontal antenna signals are added to obtain

$q(t)$.Then, $q(t)$ is downconverted by the quadrature demodulator to obtain baseband signal.Quadrature demodulator provides the inphase and quadrature components of the baseband signal to the Analog-to-Digital convertor(ADC).Then, using the complex baseband digital samples, obtained from ADC, $a(t)$ is extracted by digital signal processing.

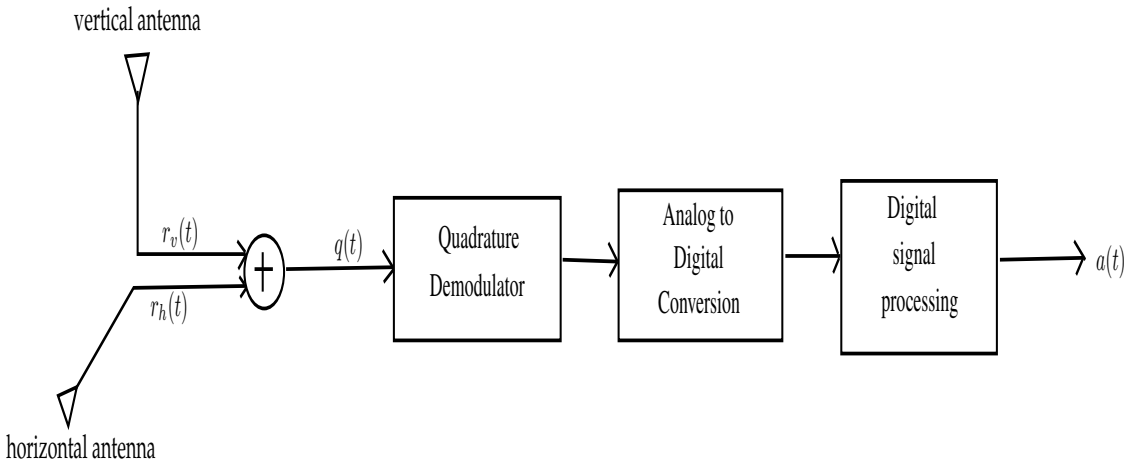

Figure 1.2: Schematic of the proposed receiver

This technique attains polarisation angle diversity but the analog signal domain manipulations performed at the transmitter require highly precise microstrip phase delay board.So, for evaluation of the polarisation angle diversity technique, an architecture was developed which produced similar rotational diversity as the proposed one, with only digital signal domain manipulations.The implementation of the experiments based on this architecture and the results are thoroughly discussed in this thesis.

1.2 Organization of the thesis

Hitachi has proposed a new radio with circular polarization as an effective solution for M-2-M communication for process industry such as oil refinery, thermal power plants and cement plants. The thesis describes the following works carried out in the project.

1. Understanding the Hitachi solution in formal signal processing language used by communications engineers, the mathematical modelling of the problem statement,

2. Building transmitters and receivers using USRPs and carry out propagation studies in environment similar to process industry

3. Developing transmitter and receiver algorithms in MATLAB and

4. The technical challenges faced during several phases of project and the solutions to overcome them.

Chapter 2 describes the offered solution under formal signal processing language used by communications engineers. Chapter 3 describes the experimental set up for gathering the data. Chapter 4 describes the technical impairments that occurred during the project such as Carrier Frequency offset, IQ imbalance and the methods to overcome them.Chapter 5 describes the transmitter and receiver signal processing algorithms used. Chapter 6 presents the analysis of the obtained observations,performance evaluation of algorithms used and conclusions.

CHAPTER 2

Signal Processing View of Polarisation Angle Diversity

Let us suppose a signal $a(t)$ is input to two synchronised modulating devices with two antennas maintained at right angles, as shown in Fig. 2.1. Let $s_v(t)$ and $s_h(t)$ be the signals at the output of the vertical and horizontal antennas. Here $s_v(t) = a(t)\cos w_1 t \cos w_c t$ and $s_h(t) = a(t)\sin w_1 t \cos w_c t$.

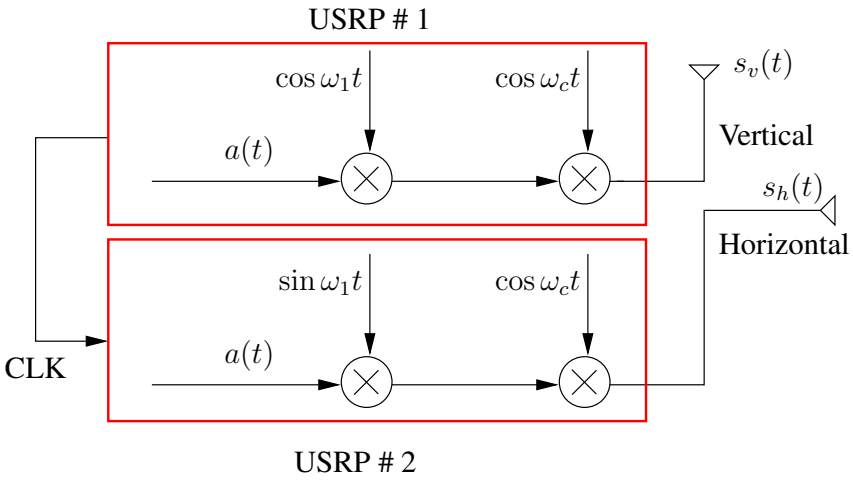

Figure 2.1: Block diagram of the transmitter

The two signal add up in space vectorially such that its projection at time t on the x-axis is $s_v(t)$ and on the y-axis $s_h(t)$. Thus the propagating signal is $a(t)\cos w_c t$. This is shown in fig 2.2. **In our experiment, w_1 and w_c are angular frequencies corresponding to 50 kHz and 460 MHz respectively** and the chip sequence,$a(t)$ is formed as shown below.

$$C = \begin{bmatrix} -1 & -1 & 1 & 1 & 1 & -1 & 1 & -1 \\ -1 & 1 & -1 & -1 & 1 & 1 & 1 & -1 \\ 1 & 1 & -1 & 1 & -1 & -1 & 1 & -1 \\ 1 & 1 & 1 & -1 & 1 & -1 & -1 & -1 \end{bmatrix},$$

where C_1, C_2 C_3 and C_4 refer to the four rows of C. $a(t)$ is formed by putting the codes C_1 to C_4 in one half cycle of w_1 and repeating it in the other half and eventually

multiplying the entire chip sequence with the sign of the bit, which is to be transmitted over that cycle of w_1.This is performed for every bit.The block code,C is formed by appending -1 to each of the four Pseudo-noise(PN-7) sequences in C_1 TO C_4.The four PN-7 sequences are chosen so that the maximum of correlations between any two rows taken, of the four rows of C, is minimum(minimax rule).Such a code,C is established by choosing a random PN-7 sequence and appending -1 to form C_1 and forming the remaining three PN sequences by circularly shifting the first PN-sequence by multiples of two.One cycle of w_1 signal spans 20 μs and thus, $a(t)$ will have a bandwidth of 3.2 MHz. **Thus, the transmission bandwidth will be 3.2 MHz**.

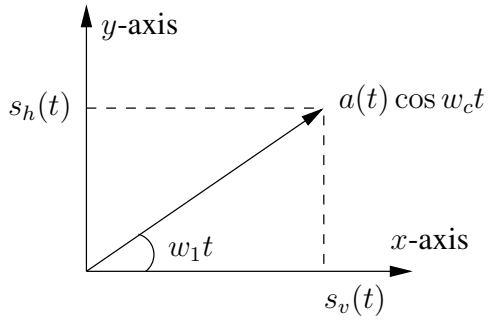

Figure 2.2: Projection of transmitted signal on to x- and y- axis

The propagating signal experiences narrowband fading due to scattering in the presence of obstruction and the received signal $r(t)$ can be written as $r(t) = h(t)a(t)\cos(w_c t + \theta(t))$, where $h(t)$ represents the narrow-band time-varying channel coefficient and $\theta(t)$ is the phase in the received signal due to the propagation time delay. This is received by a combination of vertical-horizontal antennas and a splitter as shown in fig 2.3.Narrow band fading and hence single tap channel coefficient is assumed in the project, as the distances of propagation being considered($< 100m$) are so small that all the significant multipaths have approximately the same delay as that of the Line-of-Sight(LOS) path.

The received signal $r(t)$ is projected on to vertical and horizontal antennas at the receiver generating $r_v(t)$ and $r_h(t)$ respectively as shown in fig 2.3.

Here $r_v(t) = h(t)a(t)\cos\psi(t)\cos(w_c t + \theta(t))$ and $r_h(t) = h(t)a(t)\sin\psi(t)\cos(w_c t + \theta(t))$ and $\psi(t) = w_1 t + \phi(t)$, where $\phi(t)$ is the change in angle of the received signal vector due to multipath propagation of the signal and reflections by electromagnetic scatterers. The action of the splitter is such that the carrier of $r_h(t)$ undergoes a 90^0 phase shift and the phase-shifted signal is added to $r_v(t)$. The resulting signal $q(t)$ that

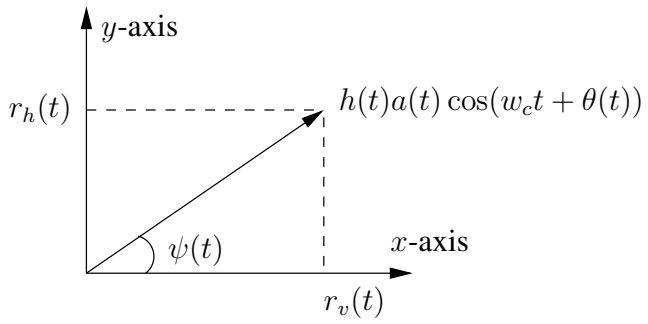

Figure 2.3: Projection of received signal onto x- and y- axes

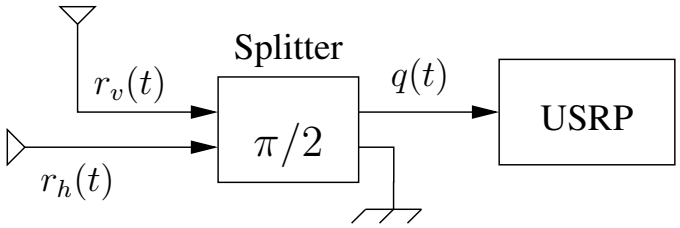

Figure 2.4: Receiver with two perpendicular antennas and a splitter

is input to the USRP is given by

$$q(t) = \underbrace{h(t)a(t)\cos\psi(t)\cos(w_c t + \theta)}_{r_v(t)} - \underbrace{h(t)a(t)\sin\psi(t)\sin(w_c t + \theta)}_{r_h(t) \text{with } 90^0 \text{ phase shift in the carrier } w_c}$$

The equivalent baseband signal $\tilde{q}(t)$ is given by

$$\tilde{q}(t) = h(t)a(t)e^{j\psi(t)} = h(t)a(t)e^{(jw_1 t + \phi(t))}$$

The problem then is given $\tilde{q}(t)$, detect $a(t)$ in the presence of fading $h(t)$.The channel fade coefficient,$h(t)$ can be estimated using a training sequence of bits in each frame as preamble and the chip sequence,$a(t)$ can be eventually extracted.The channel is assumed to be narrow-band fading single tap channel and time-invariant over a transmitted frame,which has 40 bits, in the experiments.

CHAPTER 3

Experimental Set up and Measurements

The experiment was first carried out in the *project discusion room* (room CSD 309) whose walls were covered with aluminium foil that made the walls act like a reflecting surface and an obstruction was fashioned out of the discussion board, using aluminium foil.Aluminium foil is a good reflector of electromagnetic waves and thus, can be a suitable electromagnetic scatterer,providing multipath propagations, for simulating the experiment.Also,aluminium provides good obstruction to the electromagnetic waves.The environmental setup is shown below in fig 3.1.

Figure 3.1: The experimental set up in room CSD 309

3.1 Preliminary experimental setup

The following experimental setup was used in all environments.Universal Software Radio Peripherals(USRPs) with SBX daughter boards embedded in them are used for the experiments.SBX daughter boards are used because they support Radio frequencies ranging from 400 to 4400 MHz and have low noise figure(5 dB) and give good output power(100 mW).

At the transmitter, the two USRPs are connected to a computer through ethernet cables.A MIMO(multiple input multiple output) cable is plugged into the MIMO expansion ports of the two USRPs in order to synchronize them.To each USRP,there is screwed in a 400 MHz custom antenna in the TX/RX port of the USRP.The two USRPs at the transmitter are spacially perpendicularly oriented to each other so that the antennas screwed to them are oriented perpendicularly.

Basically, the USRPs at the transmitter perform Digital to Analog conversion(DAC) on the complex digital samples which are stored in binary(.bin extension files) in the computer,upconvert and add the inphase and quadrature components of the analog signal and send the resultant signal to the antennas screwed to them.At the receiver, the USRP downconverts the received signal and stores the inphase and quadrature components of the baseband signal as digital complex samples into binary(.bin) files in the computer.

At the receiver,a USRP is connected to a computer similarly.A hybrid antenna is formed by attaching two dipole antennas perpendicularly and electrically insulated from each other.The two dipoles are connected to the two input ports of the $\pi/2$ - splitter, mentioned in chapter 2, through SMA(SubMiniature version A) cables.The 50-ohm port of the splitter is grounded and the output port is connected to the TX/RX port of the USRP through an SMA cable.

For some of the experiments carried, only a single antenna was used at the receiver which was screwed to the USRP in a similar way as transmitter.The transmitter and

receiver USRPs were supplied common 10 MHz clock signals, through the REF IN ports of the USRPs, from a Radio-Frequency(RF) generator for synchronisation.

At the transmitter, the digital samples, $a(t)\cos\omega_1 t$ and $a(t)\sin\omega_1 t$,which are stored in binary files, are supplied to the vertically and horizontally oriented USRPs by using GNU-radio companion software platform.Similarly,at the receiver the transmitted data samples are received and stored into binary files using GNU-radio companion.Before carrying out the experiment, the gains at the transmitter and receiver are adjusted by checking for clipping.Clipping is a phenomenon of the USRPs, due to which the received data is clipped to the maximum amplitude permissible for the USRP, if the transceiver gain crosses a threshold value.Clipping is checked by transmitting and receiving a sinusoidal waveform, which can be visually checked for clipping in the time domain window of the radio-companion.

3.2 Measurements in room CSD 309

The discussion room (CSD 309) was modified to have perfect reflecting wall as described above. Here the transmitter and receiver were placed 3 meters apart. A MATLAB program generates the transmitting sequence and converts the samples to .bin files needed for sending it through USRPs.

The antennas used are of 400 MHz ratings and the center frequency at which data is transmitted is 460 MHz. The transmitter has a horizontally polarized antenna and vertically polarized antenna. At the receiver for testing purpose in CSD-309 only one antenna is used whose orientations was varied from 0^0 to 90^0 in steps of 30^0 with respect to horizontal direction. As predicted, it is noticed that when receiver antenna is oriented at 0^0 only the data from horizontally polarized antenna is received and similarly at 90^0 receiver antenna orientation data from only vertically polarized antenna is received.

Also a hybrid antenna is built which has both horizontal antenna and vertical antenna,as mentioned in section 3.1, and data is received with this antenna also at receiver.

Figure 3.2: Hand made hybrid antenna

A number of different scenarios described below were realized and in each case data was recorded with and without the metallic(aluminium foil) obstruction.

Without Obstruction

1. Single transmit antenna at horizontal orientation, Single receive antenna at $0^0, 30^0, 45^0, 60^0, 90^0$ orientations with respect to horizontal direction.

2. Two transmit antennas (One horizontal and other vertical), One receive antenna at $0^0, 45^0, 90^0$ orientations with respect to horizontal direction.

3. Two transmit antennas (One horizontal and other vertical), hybrid antenna at receiver (One horizontal and one vertical).

The transmitter and receiver USRPs cannot have exactly same carrier frequency of 460 MHz. So there is a problem of Carrier Frequency Offset(CFO). For the purpose of testing, an RF frequency generator is used to give external clock to the USRPs to ensure synchronization of the USRPs. With this setup,following scenarios were setup.

Without Obstruction Two transmit antennas (One horizontal and other vertical), One receive antenna at $0^0, 45^0, 90^0$ orientations with respect to horizontal direction.

With Obstruction The following experiments are done at different obstruction spacings, *near* (0.5 m from receiver), *mid-range* (1.5 m from receiver), *far* (2.5 m from reciever).

1. Single transmit horizontal antenna, Single receive antenna at $0^0, 90^0$.

2. Two transmit (horizontal and vertical) and One receive antenna at $0^0, 90^0$

3. Two transmit (horizontal and vertical) and hybrid antenna.

The following scenarios were setup without using the external synchronizing source and repeated with and without obstruction.

- Two transmit (horizontal and vertical) antennas and receiver hybrid antenna with the obstacle placed at *near*, *mid-range* and *far* from the receiver.
- Two transmit antennas and receiver hybrid antenna without obstacle between them.

3.3 Measurement in the Machines Laboratory

The Machines Laboratory in the Electrical Engineering department was selected as the most suitable place to carry out the final measurements as this laboratory resembles a typical process industry. The laboratory is 40 m long and has a number of metal objects which function as obstructions that are so typical of a process industry. The transmitter and receiver were set up in the Machines Laboratory. Figure 3.3 shows the setup. The

Figure 3.3: The set up in the Machines Laboratory

measurements in the Machines Laboratory were carried out. The receiver was located

at a range of 30, 15 and 5 m from the transmitter. At each of these locations the transmit power was varied over two gains of 7.5 and 12.5 dB,as these were in optimum range after checking for received signal-to-noise ratio and clipping at receiver and the received samples were stored. This set up too uses two transmit antennas and at receiver a hybrid antenna.

1. In Line Of Sight (LOS) for transmitter and receiver at 5 m, 15 m and 30 m measurements were performed.

2. The measurements were repeated in NLOS situations when there is no direct path to receiver.

The following are the sample data collected(fig.3.4).There are periods of no signal in between the large amplitude frames in the figure corresponding to the zero-padding introduced between frames for the purpose of frame start timing detection.The real and imaginary parts of the baseband data received from the receiver USRP are expected to be $a(t)\cos\omega_1 t$ and $a(t)\sin\omega_1 t$ respectively.This can be seen from the fig.3.4, where the real and imaginary parts of the baseband data compensate each other in amplitudes.

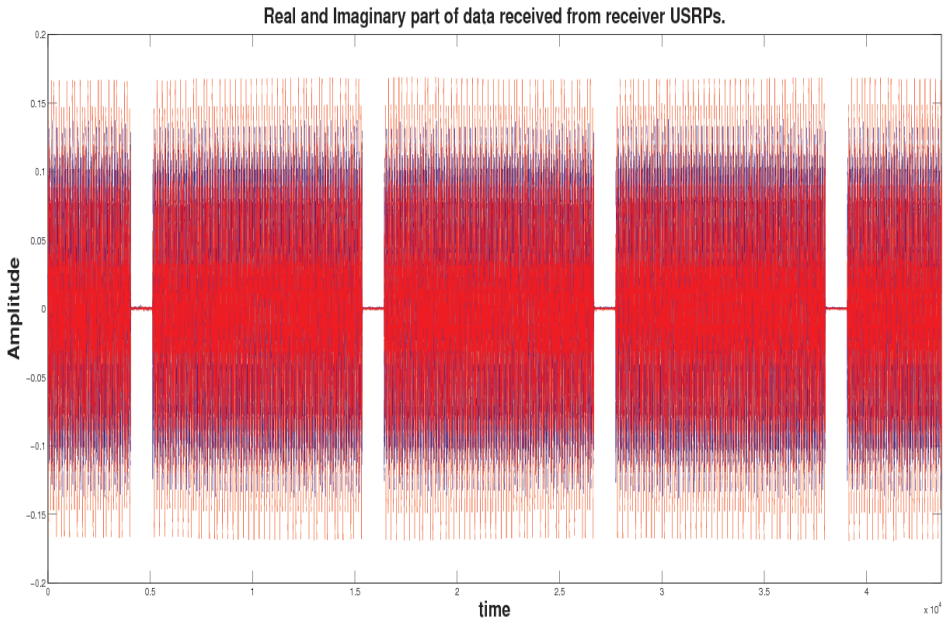

Figure 3.4: Real and Imaginary part of received data together.

CHAPTER 4

Technical impairments occurred during the project and the steps taken to mitigate them

The main impairments and the steps taken to mitigate them are as follows:

4.1 Timing Offset between rising edges of USRPs

When the two transmitter USRPs are connected by a *MIMO cable*, one of the USRPs serves as the master clock. However, this does not ensure that the rising edge of the data points are synchronized. There is indeed some offset. The two signals transmitted by USRPs are $X_1(t)$ and $X_2(t)$. If they have the timing offset then the transmitted signals are as shown.

$$\mathrm{X}_1(t) = a(t)\cos w_1 t \cos w_c t$$
$$\mathrm{X}_2(t) = a(t-\tau)\sin w_1(t-\tau)\cos w_c t$$

where τ is the timing offset between the rising edges of data samples of the two Transmitter USRPs. This eventually leads to non-synchronisation between the USRP outputs.

In order to overcome this timing offset problem the transmitter USRPs are changed from USRP-N210 to USRP-B210.Since, there is common USRP used for supplying the signals to both the transmit antennas, there is no mismatch between the timing of the rising edges of the two signals.

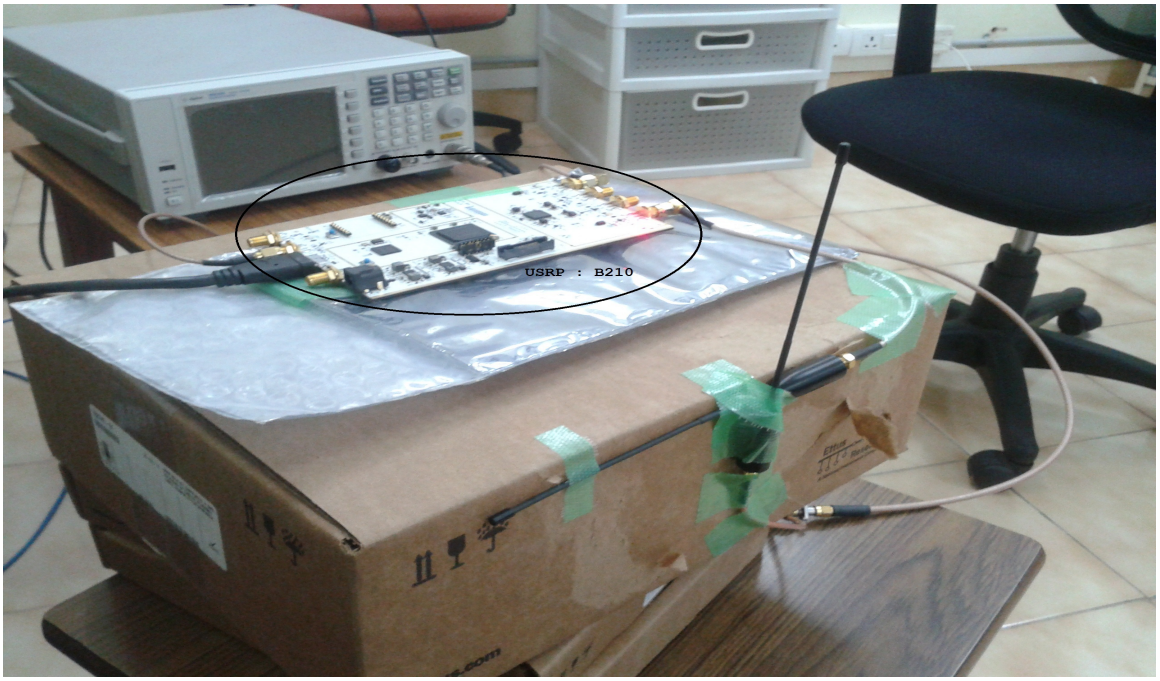

Figure 4.1: USRP B210 and the transmitting antennas

4.2 IQ Imbalance of USRP

4.2.1 Introduction

This is a severe problem in all Analog direct conversion receivers. Consider the conversion of single tone signal at RF to base band. Ideally the I and Q outputs at the receiver are

$$I(t) = cos(\omega t)$$
$$Q(t) = sin(\omega t)$$

respectively. ω is the base band frequency of the tone.With no loss of generality, we have normalized the magnitude to unity and the phase to zero, as these quantities are not relevant to this discussion. In contrast, a realistic direct conversion receiver produces:

$$I(t) = \alpha cos(\omega t) + \beta_I$$
$$Q(t) = sin(\omega t + \phi) + \beta_Q$$

where ϕ is the phase error, which we have assigned to the 'Q' path, α is the magnitude error, which we have assigned to the 'I' path, and β_I and β_Q are the DC biases

associated with each path. The allocation of error mechanisms to paths is completely arbitrary and implies no loss of generality.

Correcting β_I and β_Q is very simple. For example, β_I is simply the mean of I (t) over an integer number of periods. Given this estimate, the correction is simply a matter of subtracting β_I from the 'I' path signal. The process is the same for the 'Q' path. Then, we are left with:

$$I(t) = \alpha cos(\omega t)$$
$$Q(t) = sin(\omega t + \phi)$$

This can be rewritten in matrix form as:

$$\begin{pmatrix} I''(t) \\ Q''(t) \end{pmatrix} = \begin{pmatrix} \alpha & 0 \\ \sin(\phi) & \cos(\phi) \end{pmatrix} \begin{pmatrix} I(t) \\ Q(t) \end{pmatrix}$$

Thus we find that the correction is :

$$\begin{pmatrix} I(t) \\ Q(t) \end{pmatrix} = \begin{pmatrix} \alpha^{-1} & 0 \\ -\alpha^{-1}tan(\phi) & sec(\phi) \end{pmatrix} \begin{pmatrix} I''(t) \\ Q''(t) \end{pmatrix}$$

Thus, it remains only to findα and ϕ. To find α, define :

$$< I''(t)I''(t) >= \alpha^2 < cos^2(\omega t) >= \alpha^2 < \frac{1}{2} + \frac{1}{2}\cos(2\omega t) >= \frac{1}{2}\alpha^2 \tag{4.1}$$

and similar analysis shows that

$$< I''(t)Q''(t) >= \frac{1}{2}\alpha^2 \sin(\phi) \tag{4.2}$$

Thus the above equations are used to estimate and compensate the IQ imbalance.

4.2.2 IQ Imbalance for the data transmitted using USRPs

The RF section of a USRP has some Inphase-Quadraturephase(I-Q) imbalance which results in distortion of the complex samples as illustrated.Let us suppose the USRP is for implementation of receiver and the passband signal received is:

$$q(t) = h(t)a(t)\cos\psi(t)\cos(w_c t + \theta) - h(t)a(t)\sin\psi(t)\sin(w_c t + \theta)$$

The expected equivalent baseband signal $\tilde{q}(t)$ as USRP output is given by

$$\tilde{q}(t) = h(t)a(t)e^{j\psi(t)} = h(t)a(t)e^{j(w_1 t + \phi(t))}$$

so that,

$$Inphase[\tilde{q}(t)] = h(t)a(t)cos(w_1 t + \phi(t))$$

and

$$Quadraturephase[\tilde{q}(t)] = h(t)a(t)sin(w_1 t + \phi(t))$$

but the actual received baseband signal components due to I-Q imbalance is:

$$Inphase[\tilde{q}(t)] = \alpha\, h(t)a(t)cos(w_1 t + \phi(t))$$

and

$$Quadraturephase[\tilde{q}(t)] = h(t)a(t)sin(w_1 t + \phi(t) + \psi),$$

for some $\alpha\ \epsilon\ (-1, \infty)$.
In order to prevent this distortion,I-Q imbalance needs to be appropriately estimated for α and ψ and compensated for.

4.2.3 IQ Imbalance Compensation Using Block in GNU Radio Companion

However, in GNU radio companion this can be done by a block called 'IQ Bal Optimize'. This will estimate the IQ imbalance factors,α and ψ and removes them.

In the fig.4.2, we can observe that when IQ imbalance is not compensated an extra

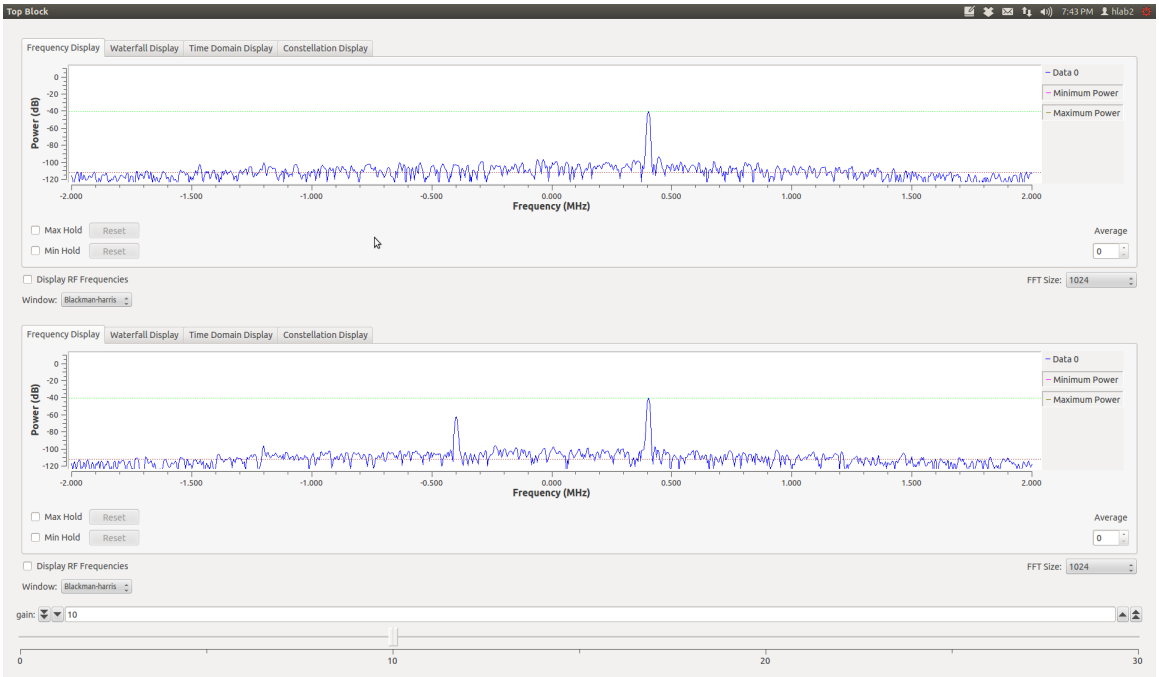

Figure 4.2: Spectrum of received signal for a transmitted single tone complex sinusoidal signal after and before IQ-imbalance compensation

tone appears when a single tone complex sinusoid is transmitted. When compensated with the block in GNU Radio Companion only the desired tone i.e the carrier is only present.For, the transmitter there is no problem of IQ imbalance while using USRP B210, since it has very negligible IQ imbalance.

4.3 Carrier Frequency offset

The clocks of the transmitter and receiver USRPs may not have same crystal frequency.Due to this, even though the USRPs are set to same carrier frequencies, there may be difference in their carrier frequencies,which can be detected using a high precision spectrum analyzer.This difference is called carrier frequency offset(CFO).For a 1ppm(parts per million) rated USRP, this offset can be at maximum one-millionth of the carrier frequency used.

There is significant carrier frequency offset(CFO) between the transmitter and receiver USRPs, which needs to be compensated.Due to the frequency offset, an extra exponential of frequency offset($e^{jw_o t}$) gets multiplied to the expected received sam-

ples.Due to this, the resultant received baseband signal is:

$$\tilde{q}(t) = h(t)a(t)e^{j(w_1 t + w_o t)},$$

where w_o is the carrier frequency offset. This carrier frequency offset is observed that it remains nearly constant over each frame(40 bits) of data received.In order to estimate the carrier frequency offset,the unwrap angle plot of $(received\ complex\ samples)^2$ for each frame of received data is linear-fitted, after removing the w_1 component from the complex samples.This estimated frequency offset(w_o) is eventually compensated for by multiplying the samples by $e^{-jw_o t}$.

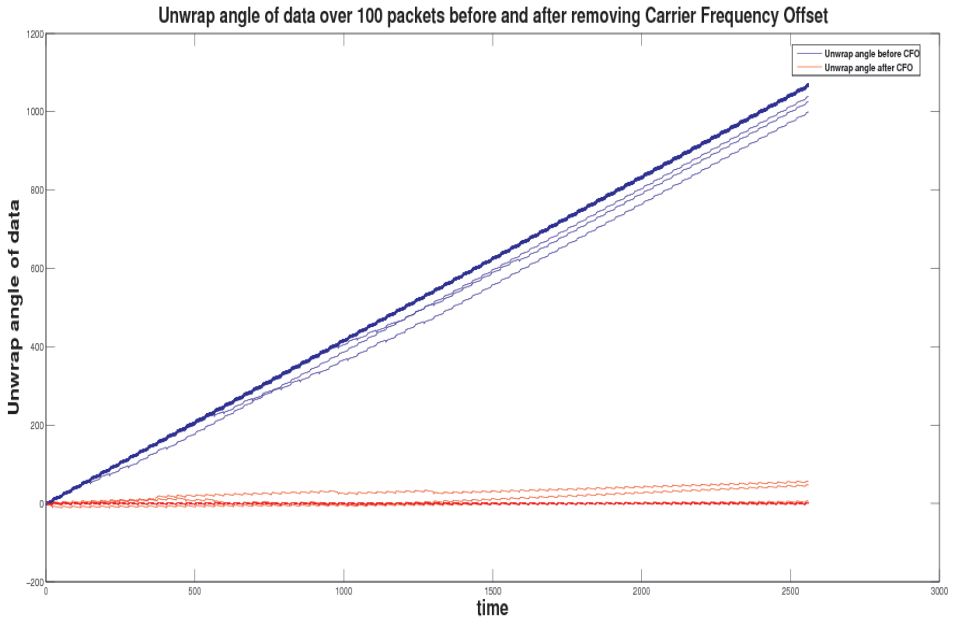

Figure 4.3: Unwrap angle plot of $(received\ complex\ samples)^2$ over several packets before and after removing Carrier Frequency Offset.

The fig.4.3 shows the unwrap angle of data over several packets before correcting for CFO and after correcting for CFO.

4.4 Frequency domain aliasing due to uncontrolled bandwidth

The 'chips' forming the block codes were used without any pulse shaping which resulted in uncontrolled bandwidth,which was greater than the sampling rate used at transmitter.This uncontrolled bandwidth resulted because there were large variations in the transmitted samples which resulted in spurious peaks.When the same sampling rate as the transmitter was used at the receiver to extract the complex samples,there was frequency domain aliasing.Thus, the bandwidth of the signal transmitted needs to be reduced.

In order to constrain the bandwidth, pulse shaping of the transmitting data is required. So Root Raised Cosine(RRC) is used as pulse shaping signal at transmitter and also used at receiver as a matched filter.Firstly, the digital signal samples at transmitter were upsampled by a oversampling factor of 4.Then, they were subjected to root-raised cosine(RRC) pulse shaping with roll-off factor of 0.2.This enabled in reducing the signal bandwidth, and thus reducing frequency domain aliasing at the receiver.The RRC pulse used is shown in fig.4.4.

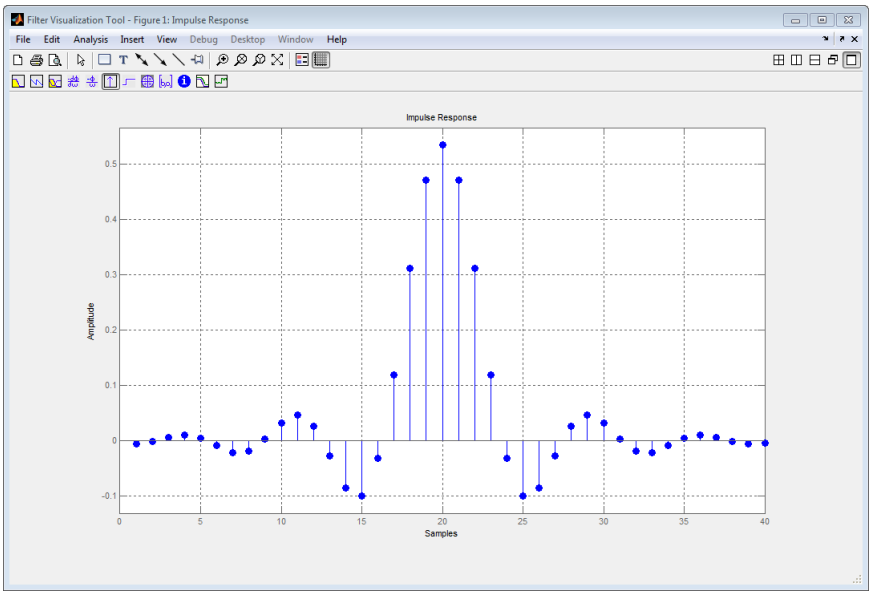

Figure 4.4: Root-raised cosine(RRC) pulse shape used with roll-off factor 0.2

CHAPTER 5

Transmitter and Receiver Algorithm in MATLAB

5.1 Transmitter

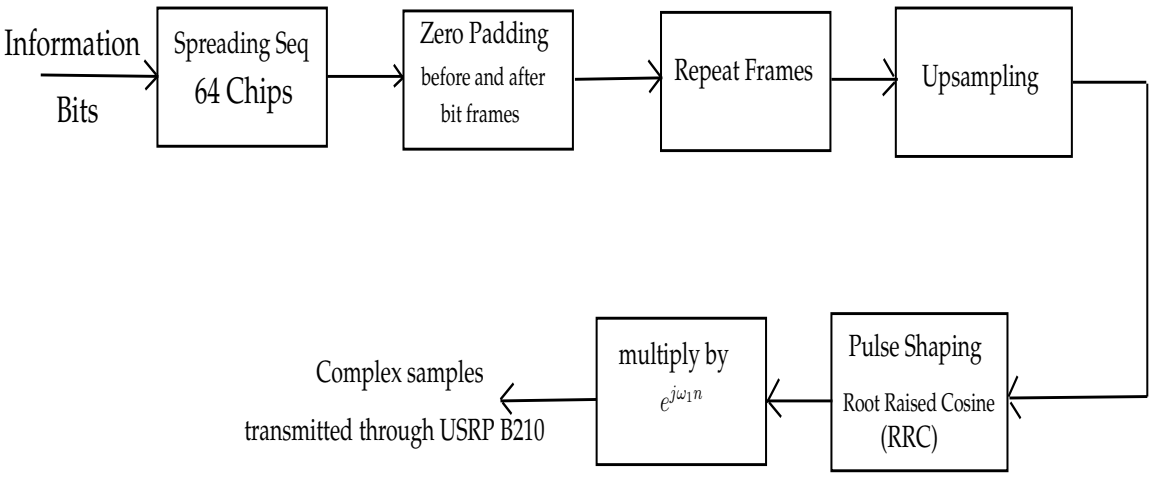

Figure 5.1: Block Diagram of the transmitter

Firstly, the information bits to be transmitted are spread using the 64-chip sequence mentioned in chapter 2.Then the frame of chips is zero padded before and after the frame.Then,the frames are upsampled by the oversampling factor of 4.Then the frames are subjected to Root-raised cosine(RRC) pulse shaping with roll-off factor, 0.2.Now, the frame is multiplied by $e^{j\omega_1 n}$ and the frames are repeatedly transmitted through the USRP B210.In our case there are two antennas transmitting at the transmitter. The connection to horizontal antenna sends upconverted $a(t)\sin(\omega_1 t)$ and the connection to vertical antenna sends upconverted $a(t)\cos(\omega_1 t)$. Then before sending signals to antennas, the USRP performs manipulations on the digital samples as mentioned in section 3.1.

5.2 Receiver

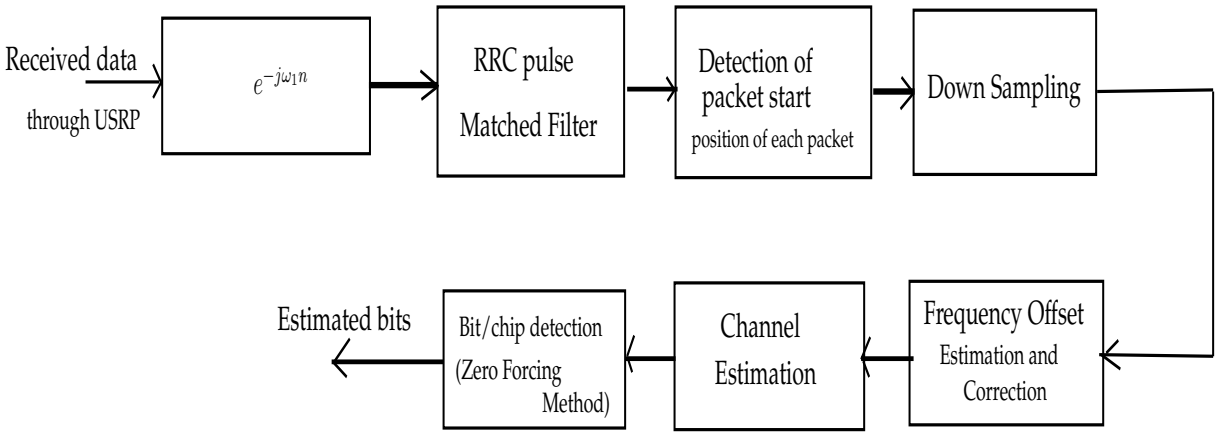

Figure 5.2: Block Diagram of the receiver

The block diagram in fig.5.2 shows the steps undertook in the receiver after the digital data is obtained from the USRPs. First the effect of $e^{j\omega_1 n}$ is removed since it is used for generating rotational polarization in antennas. Then Root-Raised Cosine(RRC) matched filter is used. For detection of data packets zero padding is done before and start of each frame. So by looking at the received data approximately the instant of start of frame is easily known.Then, the accurate start timing of frame is estimated by finding the maxima of correlation of the first three bit period complex samples with the next three bit samples which are anti-symmetric to the preceding three bits(in our experiment, the first 6 bits of the 40-bit sequence used are taken as [1 1 1 -1 -1 -1]).

Then down sampling is done by the oversampling factor of 4, to get correct number of received samples. At this stage the data should be only real. But we see complex data because of CFO between the USRPs. So CFO is removed using unwrapping algorithm.In unwrapping algorithm,the carrier frequency offset is estimated and removed by using the slope of the linear fitting of unwrap angle plot of the $(complex\ samples)^2$. Then channel is assumed to be single tap narrow band fading. First the channel is estimated taking some preamble bits. With this channel the chips(data) are found using Zero forcing method. Then the chip error rate is calculated by comparing the extracted chips with the original ones transmitted.

CHAPTER 6

Analysis of the results and algorithm performance evaluation

It was decided to externally synchronize the transmitter and receiver by RF frequency generator, so that there is independency of the results on the accuracy of the synchronization algorithms at the receiver. This allows us to focus on understanding the behaviour of polarized antennas under fading.Also USRP B210 was used at the transmitter to remove IQ-imbalance and timing offset, discussed in chapter 4.With these changes implemented in the experimental setup and the steps provided in chapter 4 implemented, the experiment was repeated in the machines lab.The data was recorded and analysed.

6.1 Channel Estimation

The channel is assumed to be narrow-band fading single tap channel.In order to estimate channel some of the starting bits of the transmitted bits are assumed to be known which act as training sequence. Using this training sequence the channel is estimated and eventually the chips and bits are recovered.The channel fade coefficient at each chip position(1 to 64)is assumed to be time-invariant over the entire length of each frame(40 bits) transmitted in the experiments.The channel is also assumed to be a single input single output(SISO) channel, where the input is $a(t)$ and the output is $y(t)$, as shown in fig.6.1.The digital signal processing block at the receiver in the diagram is clearly explained in section 5.2.

The received data after all the processing done at the receiver is

$$y(t) = h(t)a(t) + n(t)$$

where $h(t)$ is the fade coefficients,$a(t)$ is the actual signal and $n(t)$ is the noise. Using the training sequence $a(t)$ upto some time is assumed to be known. Therefore channel

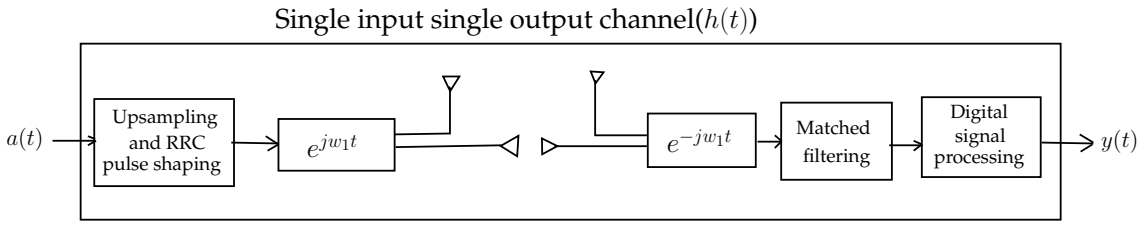

Figure 6.1: The assumed single tap channel for polarisation angle diversity.

is estimated by finding the average $h(t)$ for each chip position, averaged over the bits in the training sequence.This is the expected value of the channel fade coefficient,$h(t)$ at each chip position and thus, is the Minimum Mean Square Error(MMSE) estimate[4] of the channel fade coefficient.

Once $\hat{h}(t)$ is known $a(t)$ can be estimated as

$$\hat{a}(t) = \frac{y(t)}{\hat{h}(t)}$$

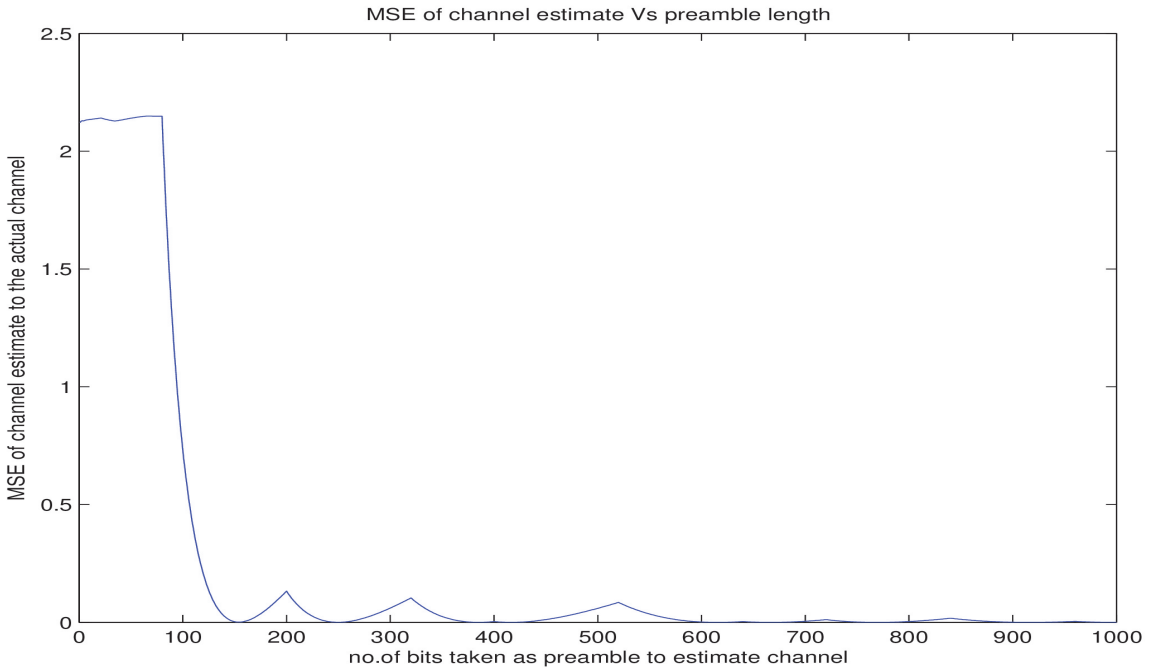

Figure 6.2: MSE between actual channel coefficients and estimated channel coefficients vs no. of bits used in training sequence.

6.2 Channel estimation for single antenna transceiver

For the purpose of comparison of results and channel fading with the traditional transceiver, experiments with environments similar to those where experiments were performed with polarisation angle diversity technique, were performed with single antenna transmitter and single antenna receiver.The transmitter and receiver antennas are aligned in the same direction.The chip sequence, $a(t)$ without any diversity, is just transmitted and received as shown in fig.6.3.

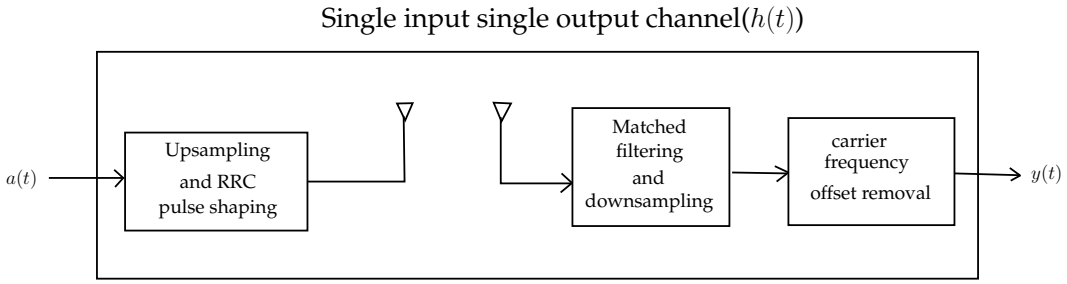

Figure 6.3: The single tap channel for single antenna transceiver.

At the transmitter, the chip sequence is upsampled by an oversampling factor 4 and then, subjected to Root-raised cosine(RRC) pulse shaping with rolloff factor,0.2 and the resultant samples are upconverted by the USRP and transmitted.At the receiver,the downconverted received samples are subjected to RRC match filtering and downsampled by the oversampling factor,4.Then,the starting instant of each frame is estimated and each frame of samples is subjected to carrier frequency offset removal.The resultant sample sequence is $y(t)$.

Even here, the channel is assumed to be single tap narrow band fading and time-invariant over each transmitted frame of 40 bit length.The channel is also assumed to be a single input single output channel.So, the same channel equation as that used for polarisation angle diversity can be used.Thus, the channel fade coefficients,$h(t)$ for various chip positions are estimated in the same way as that for polarisation angle diversity technique.

6.3 Comparison of channel fade Coefficients as seen by polarised and single antenna transceivers

The averaged $|h(t)|^2$(where $h(t)$ is the narrow-band channel fade coefficient) obtained after the signal processing, is plotted as a function of 64 chips.The averaging is done over 100 packets (each packet containing 40 bits i.e. 2560 chips).

Figures 6.4 to 6.7 compare the average fade coefficient $|h(t)|^2$ for the two scenarios, the case that uses the polarization angle diversity(polarised),shown in blue colour, and the case that uses single antenna both at the transmitter and the receiver,shown in red, and the comparison is done for both Line-of-sight(LOS) and non line-of-sight(NLOS) metallically obstructed propagation path scenarios.The x-axis shows the chip position number out of 64 chips forming a bit.

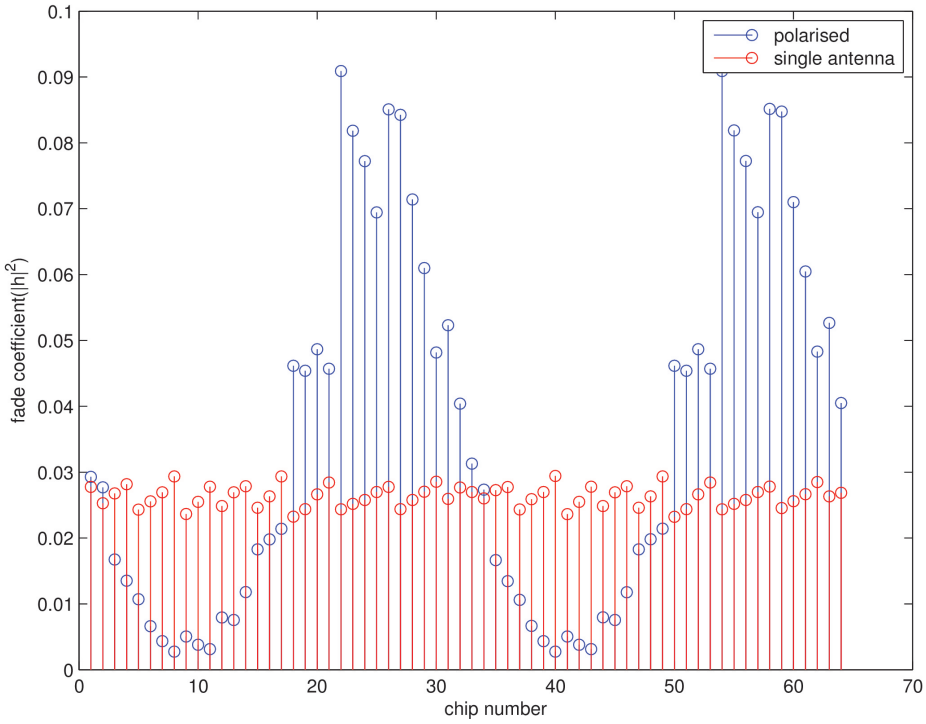

Figure 6.4: Comparison of fade coefficients as seen by polarised angle diversity and single antenna transceivers under an LOS scenario.

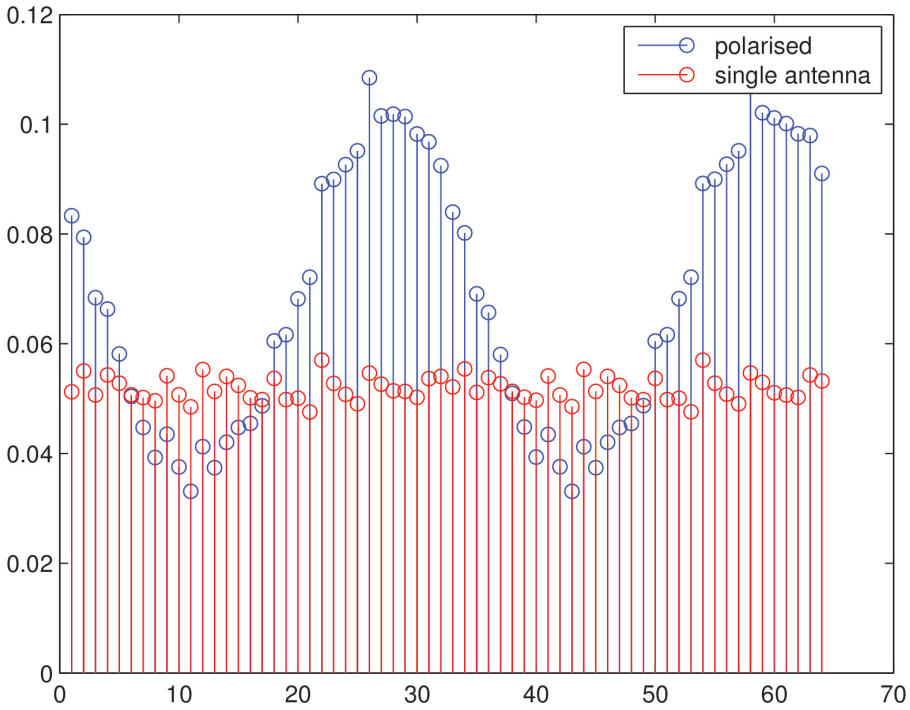

Figure 6.5: Comparison of fade coefficients as seen by polarised angle diversity and single antenna transceivers under another LOS scenario.

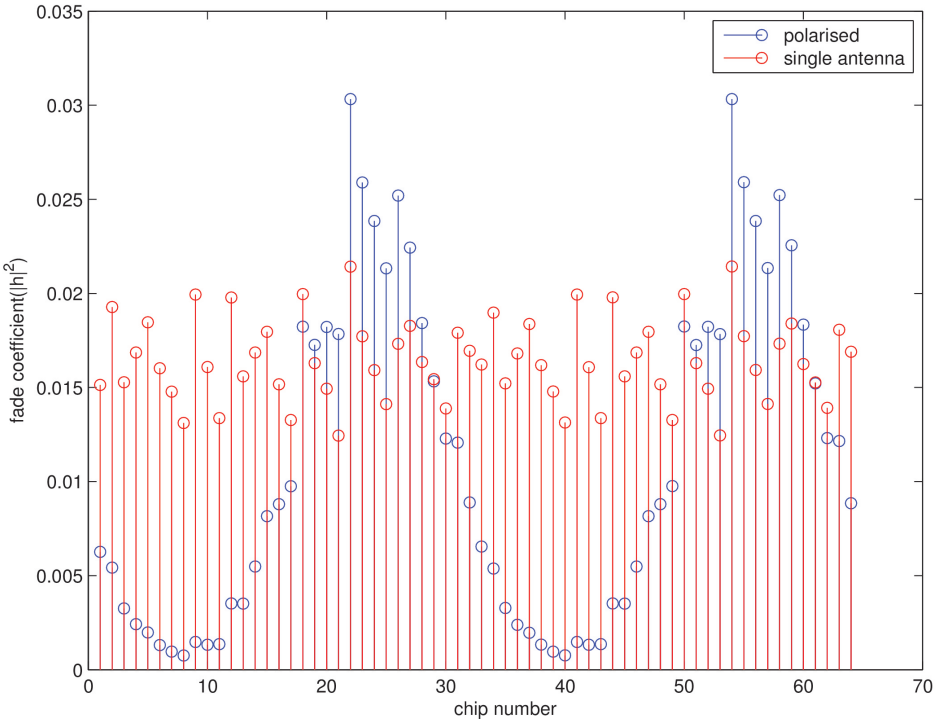

Figure 6.6: Comparison of fade coefficients as seen by polarised angle diversity and single antenna transceivers under an NLOS(non line-of-sight) scenario.

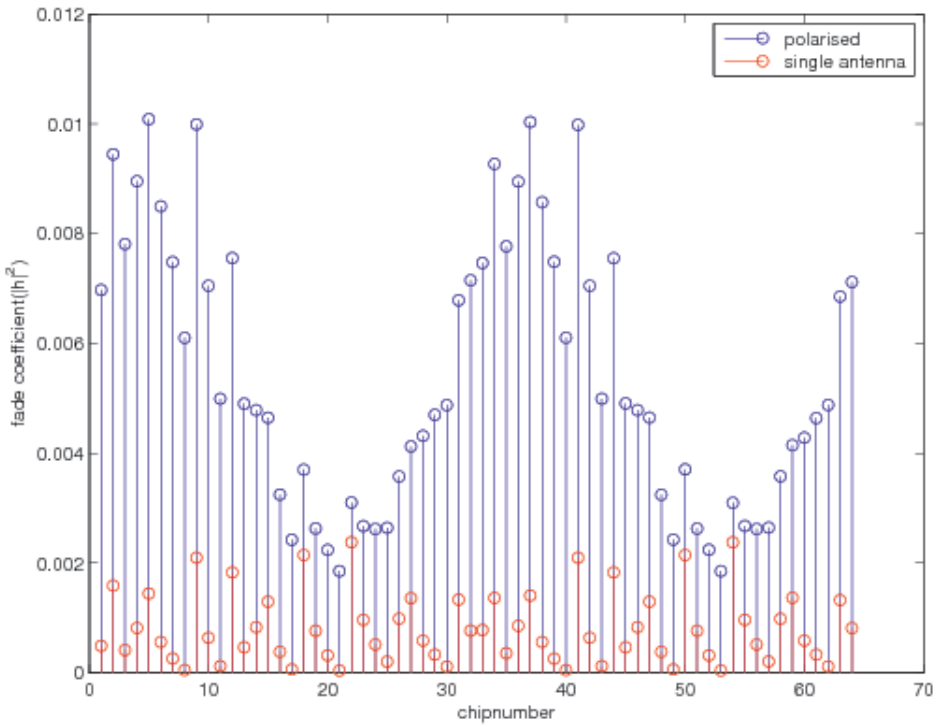

Figure 6.7: Comparison of fade coefficients as seen by polarised angle diversity and single antenna transceivers under another NLOS(non line-of-sight) scenario.

We can clearly observe from the plots that in the case of single antenna transceiver, all the chip positions undergo similar fading by the channel.So,whenever there is a deep fade and channel outage, all the chips undergo outage and so all chip positions suffer similar high average chip error probability.This leads to slow fading.

Whereas, in polarisation angle diversity technique, there is fast and shaped channel fading occurring.There are chip positions where the channel better even when the average channel fade coefficient is below outage threshold.Due to this, even when many chips cannot be recovered accurately due to outage, atleast some of the chips where channel is good, can be recovered precisely.Using these accurately estimated chips, we can extract the information bits from the received samples very precisely, with lower bit error rate as compared to the traditional transceiver setup.

The channel fading experienced by a particular chip is based on its position from 1 to 64,.i.e it is based on the polarisation angle with which it was transmitted at the transmitter.In the case of single antenna transceiver,all the chip positions experience similar channel.But due to polarisation angle diversity, various chip positions are transmitted

at various polarisation angles resulting in different multipath channels.So,even when, at an instant, the multipath channel is very obstructive to the signal, at another instant at different polarisation angle,the multipath channel may be conducive and favourable for propagation.

The channel fade coefficient is periodic with 32-chip period because the spreading block code(block code C in chapter 2) and the polarisation angle of transmission and thus the channel is periodic with fundamental period of 32 chips.The channel has lower probability in the polarisation angle diversity case of going into outage for all chip positions.Therefore, the polarisation angle diversity technique implemented in the project is beneficial in highly electromagnetic scattered environment like industries where highle reliable communication among the infrastructure is expected.

6.4 Performance evaluation of receiver algorithm

The polarisation angle diversity transceiver algorithm was simulated in MATLAB.After obtaining the transmitter complex samples for a large number of frames,say 1000, by the transmitter algorithm mentioned earlier, the samples were subjected to complex additive white gaussian noise as shown in the equation below:

$$y[n] = s[n] + w[n],$$

where y[n] is the received sample,s[n] the transmitted sample and w[n] is the additive gaussian noise.The SNR of the simulated AWGN channel is varied from 0 to 20 dB.

Then the received samples are subjected to carrier frequency offset(Fo) at the receiver.With the transmitter and receiver USRPs both having 5ppm(parts per million) error rated crystal oscillators,the worst case carrier frequency offset arises when there is 10 ppm offset between them.In this case,for a carrier frequency of around 400 MHz used,there is carrier frequency offset of 4KHz.The simulations are performed with Fo taking values as 4 KHz(which is worst case frequency offset for 5 ppm USRP at center frequency 400MHz),8 KHz(for 10 ppm USRP),12 KHz(15 ppm USRP) and 16 KHz(20 ppm USRP).

Then, the chips are recovered using the receiver algorithm mentioned earlier.The mean square error of the estimated frequency offset,averaged over the 1000 frames used, is obtained by comparing the frequency offset, estimated by the technique mentioned in receiver algorithm, with the actual frequency offset introduced.The plot for logarithm of mean square error of estimated carrier frequency offset(in radians/sample at sampling frequency 2MHz)for Signal to Noise ratio of the AWGN channel varying from 0 to 20 dB is shown below in fig.6.8.

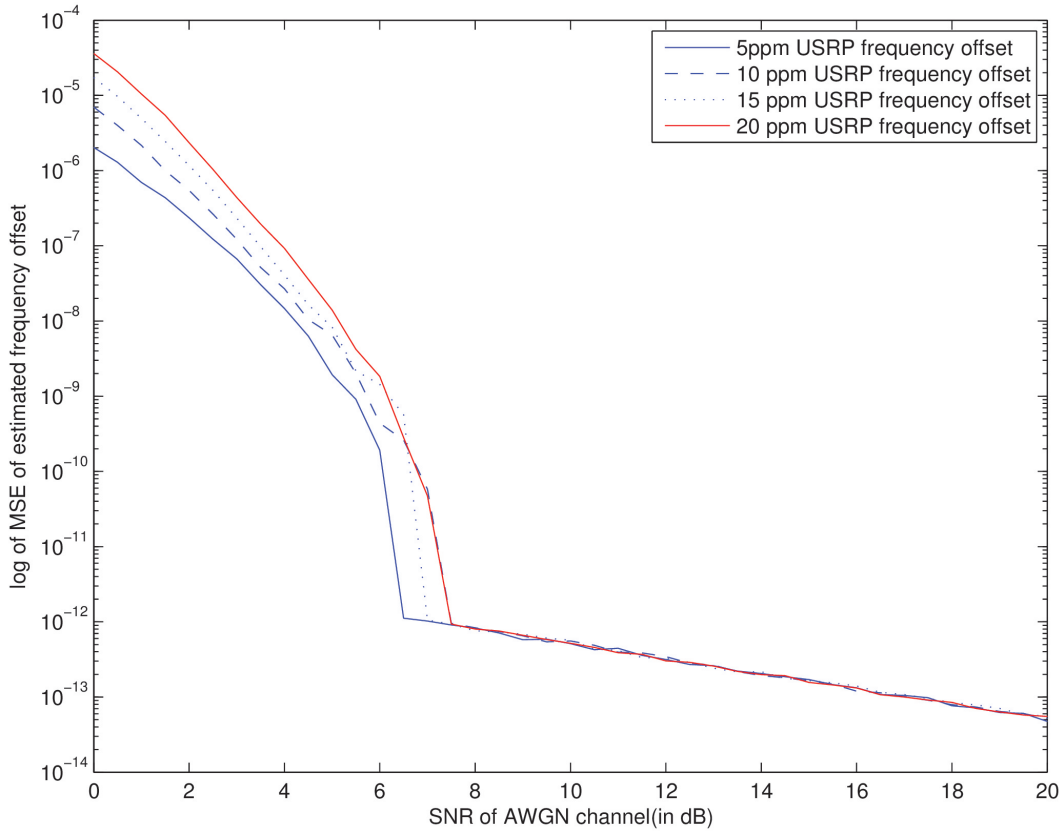

Figure 6.8: Logarithm of mean square error of estimated frequency offset(in radians/sample at sampling frequency 2MHz) vs Signal-to-Noise ratio(SNR) of AWGN channel(in dB) for worst case frequency offset for 5, 10, 15 and 20 ppm USRPs.

The mean square error of the estimated frame-start timing by the method mentioned in the receiver algorithm, averaged over 1000 frames,is also obtained for the various frequency offsets introduced.The plot for logarithm of mean square error of estimated frame-start timing for Signal to Noise ratio of the AWGN channel varying from 0 to 20 dB is shown below in fig.6.9

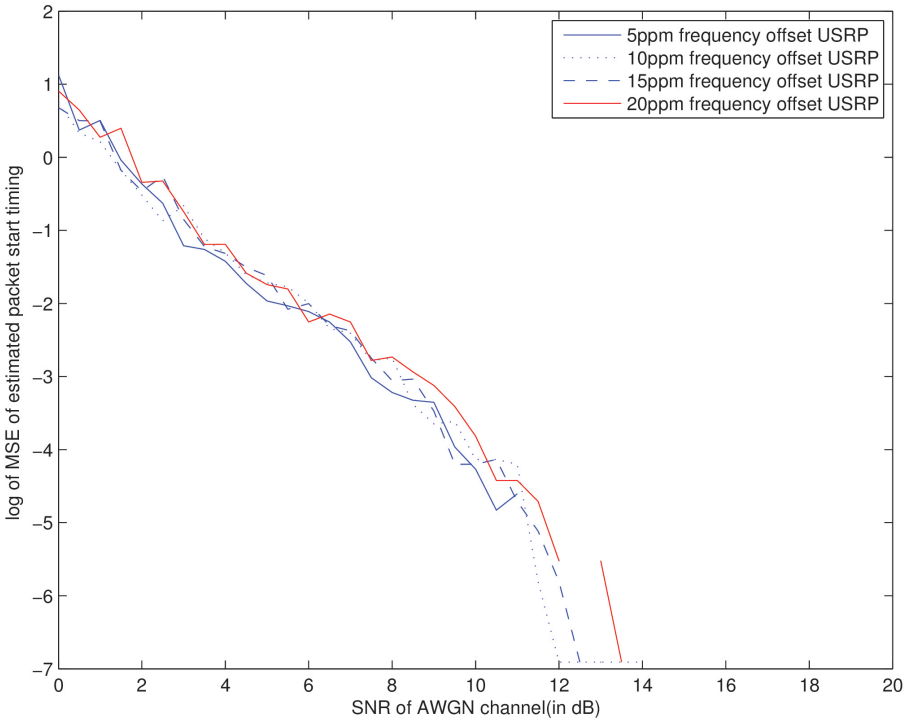

Figure 6.9: Logarithm of mean square error of estimated frame-start timing vs Signal-to-Noise ratio(SNR) of AWGN channel(in dB) for worst case frequency offsets for 5, 10, 15 and 20 ppm USRPs.

6.5 Chip Error Rate curve

As the data is obtained over many distances in the practical environment, with the increase in distance between the transmitter and receiver the chip error rate increases because of fading, attenuation, AWGN noise. In our case the noise is very less in the received data. So we have simulated AWGN in matlab and is added to the data with appropriate SNRs. Then channel estimation is done to know $h(t)$ and zero forcing equalizer is used to find the bits and finally chip error rates.The chip error probabilities are found by comparing the estimated chips, $\hat{a}(t)$ with the actual transmitted chips, $a(t)$ and then averaging this absolute error over all the frames received.

The theoretical and experimental average chip error rate,averaged over several frames,for the polarisation angle diversity technique for varying SNR(in dB) of the AWGN added is shown in fig. 6.10 .

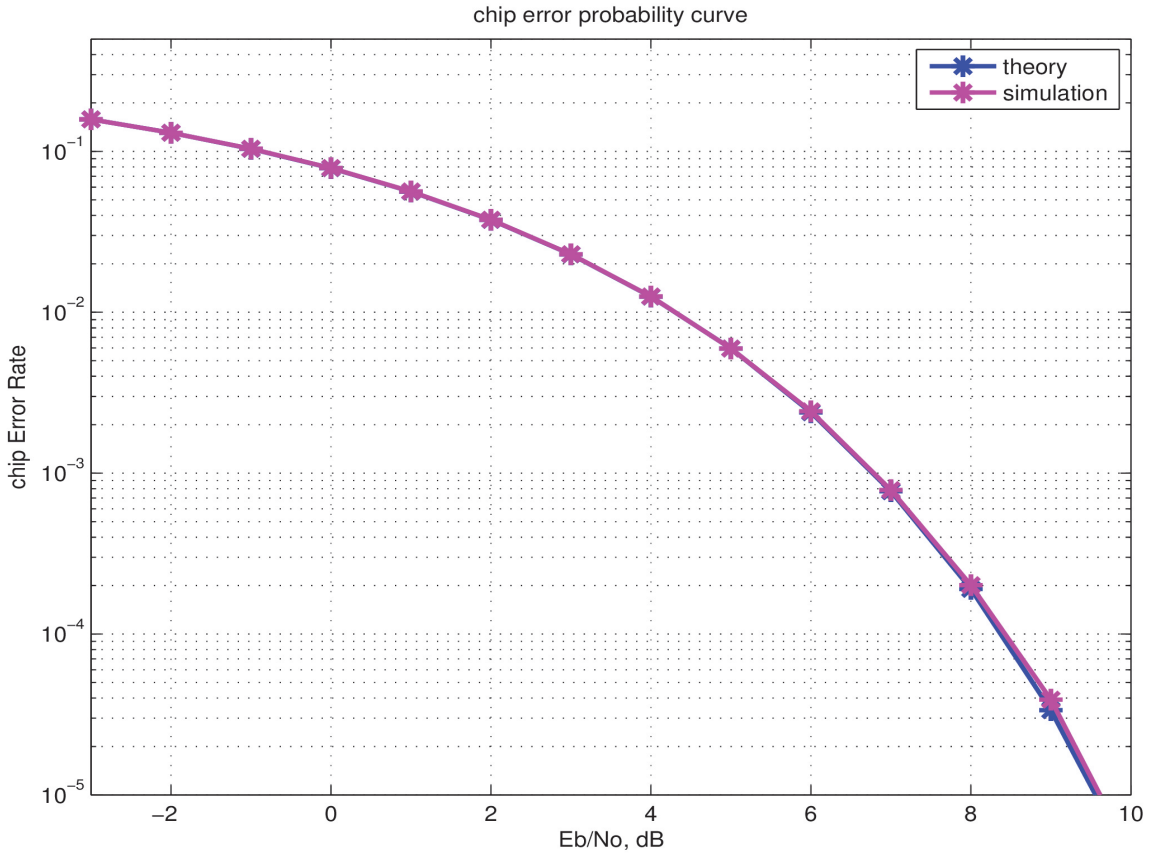

Figure 6.10: Chip Error Rate vs SNR

CHAPTER 7

Conclusions

The following are the conclusions inferred from the project:

1. The preliminary results of the experiment suggest that use of Hitachi polarized antennas results in shaping of the fading environment. These initial results shows rotational polarization in action and we see that the fading seen by a particular chip is based on the polarization it experiences.

2. From the figures 6.4 to 6.7,we can see that unlike single antenna transmitter and receiver setup,where there is slow constant fading over time,the polarisation angle diversity technique enables fast and shaped fading.Due to this,we can extract the information bits efficiently by considering the chip positions where the channel is better.Thus this technique turns out to be advantageous in highly electromagnetic scattered environment like industries where highly reliable and secure communication among the infrastructure is expected.

3. Frequency synchronization is very critical to the working of the system. Unlike other single-carrier systems, we deliberately multiply the signal with a complex exponential to induce circular polarization and this is of the order of few KHz. Hence the carrier frequency offset should be much less than the KHz range for the system to operate correctly.

4. Pulse shaping with an RRC pulse and an appropriate bandwidth expansion factor is absolutely necessary for the system to work. Without pulse shaping, the receiver ADC would be required to operate at a much higher bandwidth with low-pass filtering. This is mainly to prevent frequency domain aliasing and ISI caused by the infinite bandwidth of the square pulses being transmitted.

CHAPTER 8

References

[1] *'Polarization angle diversity for highly-reliable Machine-to-Machine radio'*, by Dr. Ken Takei.

[2] *'Design and analysis of transmitter diversity using intentional frequency offset for wireless communications'*, by Wen-Yi Kuo and Michael P.Fitz, members of IEEE.

[3] *'Combined effects of phase sweeping transmitter diversity and channel coding'*, by Akira Hiroike, Fumiyuki Adachi and Nobuo Nakajima, members of IEEE.

[4] Chapter 11 of *'Fundamentals of Statistical Signal Processing - Estimation Theory'*, by Steven M Kay.

APPENDIX

The following is the MATLAB code for the transmitter:

```
run /parameters  %parameters extracted from parameters code
frame = [];
frame2=[];
tt=[];

%%Spreading by 64 chip sequence
for k=1:bits_per_frame
    frame =[frame bits(k)*chip_seq];
    frame2 =[frame2 bits(k)*chip_seq];
    tt =[tt bits(k)*chip_seq];
end

%Zero padding before and after the frame
frame = [zeros(1,pre_post_zeros*chips_per_bit) frame zeros(1,pre_post_zeros*chips_per_bit)];
frame = scale_factor*frame;

%repeating the same frame, total_no_frames times

frame_tx_pre_rrc=repmat(frame,1,total_no_frames);

%%Upsampling and root-raised cosine(RRC) pulse shaping
%fvtool(hd, 'impulse')  is used to generate the RRC filter impulse response, hd
filter_tx = hd.numerator;
frame_over_sampled  = upsample(frame_tx_pre_rrc,over_sampling_factor);
frame_rrc_tx_pre_exp = conv(filter_tx, frame_over_sampled);

%Multiplying by exp{j(w1)n}
frame_rrc_tx =  frame_rrc_tx_pre_exp.*exp(1i*2*pi*(1:1:length(frame_rrc_tx_pre_exp))/
(chips_per_bit*over_sampling_factor));

% Store in the appropriate files
 csvwrite('/home/hlab7/project/hitachi_exp_apr16/transmit_cos',real(frame_rrc_tx.'));
 csvwrite('/home/hlab7/project/hitachi_exp_apr16/transmit_sin',imag(frame_rrc_tx.'));
```

The following 'parameters' MATLAB code contains the various parameters used and is run in the transmitter and receiver codes :

```
bits_per_frame =40;
chips_per_bit=64;
pre_post_zeros= 2;  % No. of zeros to be added before and after the actual data
scale_factor =0.5;%to be multiplied with the frame to be transmitted
total_no_frames =10;

%RRC pulse shaping
over_sampling_factor = 4
symbol_durations =12;
roll_off=0.2 ;

%sampling rate of USRPs
usrp_tx_sampling_rate =2e6;
usrp_rx_sampling_rate = 2e6;

%decimation and interpolation factors
if(usrp_tx_sampling_rate > usrp_rx_sampling_rate)
    decim_fac = usrp_tx_sampling_rate/usrp_rx_sampling_rate;
    interp_fac =1;
else
    interp_fac=usrp_rx_sampling_rate/usrp_tx_sampling_rate;
    decim_fac =1;
end

% receiver parameters.
% The following are used as preamble to find the start of the frame.
no_bits_time = 6;
bit_timing =[ 1 1  1 -1  -1 -1 ];% observe the anti symmetry.

% For locking to the correct RC sample;
oversampling_time_phase =4;
hsync = comm.GardnerTimingSynchronizer('SamplesPerSymbol',
oversampling_time_phase*over_sampling_factor*interp_fac/decim_fac, 'ErrorUpdateGain', 0.007);
```

```
% Transmitter
h  = fdesign.pulseshaping(over_sampling_factor,'square root raised
cosine','nsym,beta',symbol_durations,roll_off);
hd = design(h);

% Receiver
%% rrc filtering at the receiver. however the rates should match
over_sampling_factor_rx =over_sampling_factor*interp_fac/decim_fac;
h2  = fdesign.pulseshaping(over_sampling_factor_rx,'square root raised
cosine','nsym,beta',symbol_durations,roll_off);
hd2 = design(h2);

%Block code, C
code0=[-1 -1 1 1 1 -1 1 -1;
       -1 1 -1 -1 1 1 1 -1;
       1 1 -1 1 -1 -1 1 -1;
       1 1 1 -1 1 -1 -1 -1];
  code1=[];
  for i=1:4
      code1=[code1,code0(i,:)];
  end
chip_seq=[code1 code1];
%Bits.mat is a file where the bit sequence used for experiments is stored.
bit_file = load('Bits.mat');
bits = bit_file.Bits;
```

The following is the MATLAB code for receiver:

```
run /home/hlab10/project/hitachi_exp_apr16/receiver/parameters
%% usrp receiver
usrp_out1=read_complex_binary('april22_6m_highNLOS_sync_2MHz.dat');
usrp_out1= usrp_out1.';

%% Removing the multiplied exp{j(w1)n}
usrp_out=usrp_out1.*exp(-1i*2*pi*(1:1:length(usrp_out1))/
(chips_per_bit*over_sampling_factor*interp_fac/decim_fac));

%Match filtering
filter_rx = hd2.numerator;
frame_rrc_rx = conv(usrp_out,filter_rx);

samples_per_bit=over_sampling_factor*chips_per_bit*interp_fac/decim_fac;
frame_size_rx = bits_per_frame*over_sampling_factor*chips_per_bit*interp_fac/decim_fac;
zeros_frame_size = pre_post_zeros*2*over_sampling_factor*chips_per_bit*interp_fac/decim_fac;
signt = repmat(bit_timing,samples_per_bit,1);
sign_mul = signt(:).';


chip_error = zeros(total_no_frames,1);
start0 = 10008026; % rough estimate of frame start timing
no_packets =100

start =start0
chip_err=[];
for m=1:no_packets
    m
    %% we now do the timing recovery of start of each frame
%%we look  for anti-symmetry.
    metric =[];
 for k=start-1000:start+1200
        window = frame_rrc_rx(k:k+(samples_per_bit*no_bits_time-1)).*sign_mul;
                    metric = [metric
sum(window(1:samples_per_bit*no_bits_time/2).*conj(window((samples_per_bit*no_bits_time/2)+1:
samples_per_bit*no_bits_time)))];
    end
```

```
    [mm,pos]= max(abs(metric));
    frame_start_pos = start + pos-1001;
    winde=frame_rrc_rx(frame_start_pos:frame_start_pos+(frame_size_rx));
    start = frame_start_pos+frame_size_rx+zeros_frame_size;

    frame_rx = frame_rrc_rx(frame_start_pos:(frame_start_pos+frame_size_rx-1));
    frame_rx = frame_rx -mean(frame_rx);

    %% oversampling for timing phase recovery.
    frame_rx_interp = interp(frame_rx,oversampling_time_phase);
    [~, phase] = step(hsync,frame_rx_interp.');
    pos_start = round(phase(end))+1;

%% we now downsample and finally extract the original frame
    packet = frame_rx_interp(pos_start:
oversampling_time_phase*over_sampling_factor*interp_fac/decim_fac: end);

%%Frequency offset estimation and removal
    xx=(1:length(packet))';
    coef = polyfit(xx,(unwrap(angle(packet.^2)))',1);
    dat_unrot1 = (packet).*exp(-1i*((0.5*coef(1))*(1:1:length(packet))  +0.5*coef(2)));

    plot(unwrap(angle(packet.^2))); hold on;
    plot(unwrap(angle(dat_unrot1.^2)),'r');
    legend('Unwrap angle before CFO','Unwrap angle after CFO');

    chip_err = [chip_err    real(dat_unrot1)];
    dat_unrot1_concat = chip_err;
end

%% Channel Estimation Algorithm

no_of_bits = 1000;

tt1= [];
tt_concat = [];
for i = 1:100
    tt_concat = [tt_concat tt];
end
```

```
h_actual = dat_unrot1_concat(1:no_of_bits*64).*tt_concat(1:no_of_bits*64);
h_actual_avg = zeros(1,64);

for i=1:64
for k=1:no_of_bits
h_actual_avg(i)=h_actual_avg(i)+h_actual((k-1)*64+i);
end
end
h_actual_avg = h_actual_avg/no_of_bits;

%plot of channel fade coefficient(|h(t)|^2)
figure;
stem(h_actual_avg.^2);
title('|h_actual_avg|^2');

MS_error = zeros(1,no_of_bits);
%Preamble1 is the no.of bits taken as training sequence for channel estimation
for Preamble1 = 1:no_of_bits
h_estimate_avg = zeros(1,64);
h_estimate = dat_unrot1_concat(1:Preamble1*64) .* tt_concat(1:Preamble1*64);
for i=1:64
for k=1:Preamble1
h_estimate_avg(i)=h_estimate_avg(i)+h_estimate((k-1)*64+i);
end
end
h_estimate_avg = h_estimate_avg/Preamble1;

MS_error(Preamble1) = sum((h_actual_avg - h_estimate_avg).^2);
end

%plot of mean square error of channel estimation vs training sequence length
figure;plot(MS_error);

%chip detection for each frame
h_est = [];
for k = 1:40 %frame of 40 bits
    h_est = [h_est h_estimate_avg];
end
```

```
    decoded_chips_best_estimate =2*(real(dat_unrot1)./h_est)*6>0-1;
    if(decoded_chips_best_estimate(1)*tt(1) <0)
        decoded_chips_best_estimate = -1*decoded_chips_best_estimate;
    end

%No. of chip errors in each detected frame
chip_error = nnz( decoded_chips_best_estimate - real(tt(1:length(decoded_chips_best_estimate))))
end
```